The Stability, Structural Organization, and Denaturation of Pectate Lyase C, a Parallel β-Helix Protein†

Douglas E. Kamen,‡ Yuri Griko,§ and Robert W. Woody*,‡

Department of Biochemistry and Molecular Biology, Colorado State University, Fort Collins, Colorado 80523, and Department of Biology, The Johns Hopkins University, Baltimore, Maryland 21218-2685

Received August 11, 2000; Revised Manuscript Received October 23, 2000

ABSTRACT: Pectate lyase C (pelC) was the first protein in which the parallel β-helix structure was recognized. The unique features of parallel β-helix-containing proteins—a relatively simple topology and unusual interactions among side chains—make pelC an interesting protein to study with respect to protein folding. In this paper, we report studies of the unfolding equilibrium of pelC. PelC is unfolded reversibly by gdn-HCl at pH 7 and 5, as monitored by far- and near-UV CD and fluorescence. The coincidence of these spectroscopically detected transitions is consistent with a two-state transition at pH 7, but the three probes are not coincident at pH 5. No evidence was found for a loosely folded intermediate in the transition region at pH 5. At pH 7, the $\Delta G^{\circ}_{H_2O}$ for unfolding is 12.2 kcal/mol, with the midpoint of the transition at 0.99 M gdn-HCl and $m = 12.3$ kcal/(mol·M). Thus, pelC is unusually stable and has an m value that is much larger than for typical globular proteins. Thermal denaturation of pelC has been studied by differential scanning calorimetry (DSC) and by CD. Although thermal denaturation is not reversible, valid thermodynamic data can be obtained for the unfolding transition. $\Delta H_{van't\ Hoff}/\Delta H_{cal}$ is less than 1 for pHs between 5 and 8, with a maximum value of 0.91 at pH 7 decreasing to 0.85 at pH 8 and to 0.68 at pH 5. At all pHs studied, the excess heat capacity can be deconvoluted into two components corresponding to two-state transitions that are nearly coincident at pH 7, but deviate more at higher and lower pH. Thus, pelC appears to consist of two domains that interact strongly and unfold in a cooperative fashion at pH 7, but the cooperativity decreases at higher and lower pH. The crystal structure of pelC shows no obvious domain structure, however.

A fundamental aim in biological sciences is to understand the mechanism by which a protein adopts its functional three-dimensional structure. Studies on small model proteins such as lysozyme, myoglobin, and α-lactalbumin have led to significant advances toward this aim. A type of protein fold known as the parallel β-helix, first reported in 1993, has been observed in several proteins (*1*−*6*). The first to be observed, and the focus of this study, was pectate lyase C (pelC)[1] from *Erwinia chrysanthemi* (*1*, *2*). PelC is a virulence factor among the causative agents thought to be responsible for soft-rotting disease of plant tissue (*7*, *8*). PelC and other pel isozymes depolymerize polygalacturonides in the presence of Ca^{2+} ions, effectively destroying the integrity of plant tissues (*7*). The pel enzymes catalyze the cleavage of the α-1,4-glycosidic linkages in pectate (*7*). Cleavage proceeds via a β-elimination mechanism (*7*, *9*), predominantly resulting in trisaccharides, and rarely disaccharides and tetrasaccharides.

PelC is a single polypeptide chain of 37 676 Da that apparently consists of a single domain. The structure of pelC, which has been determined by X-ray crystallography at 2.2 Å resolution, is shown in Figure 1 (*1*). A notable feature of this structure is the relatively high parallel β-sheet content making up the dominant fraction of the secondary structure (Table 1). The most interesting characteristic of the polypeptide backbone is that these parallel β-sheets wind up to form a large right-handed coil, called a parallel β-helix. This makes a very simple and highly ordered topology that went unobserved and unpredicted in more than 30 years of protein crystallography and nuclear magnetic resonance spectroscopy. Each of the three sheets, labeled PB1−3, is composed of 6−10 strands, and together they form 7 complete turns of the β-helix. PelC contains about 30% parallel β-sheet (Table 1), thus making it a good system to study the folding and structural organization of this type of secondary structure.

In addition to the unique backbone topology, pelC contains several unusual side-chain interactions. The hydrophobic core contains several stacks of interdigitated aliphatic residues. The stacks contain from 3 to 10 residues each and total 108 interacting branched-chain residues. Connecting two of the sheets (PB2 and PB3) is a rare $\gamma\beta_E$ turn. In six of these turns, one residue is always an asparagine, making a ladder of asparagine residues inside the core of the protein. There is a second polar amino acid stack inside another turn (between sheets PB1 and PB2) comprised of three serine residues. In

† Supported by USPHS Grant GM-22994.

* Correspondence should be addressed to this author. E-mail: rww@lamar.colostate.edu, fax: 970-491-0494.

‡ Colorado State University.

§ The Johns Hopkins University.

[1] Abbreviations: pelC, pectate lyase C; DSC, differential scanning calorimetry; UV, ultraviolet; CD, circular dichroism; LB, Luria−Bertani; IPTG, isopropyl-β-D-thiogalactopyranoside; M_r, relative molecular mass; SDS−PAGE, sodium dodecyl sulfate−polyacrylamide gel electrophoresis; HPLC, high-pressure liquid chromatography; gdn-HCl, guanidine hydrochloride; ANS, 8-anilino-1-naphthalenesulfonate; PP_{II}, poly(proline) II.

10.1021/bi001900v CCC: $19.00
Published on Web 11/30/2000

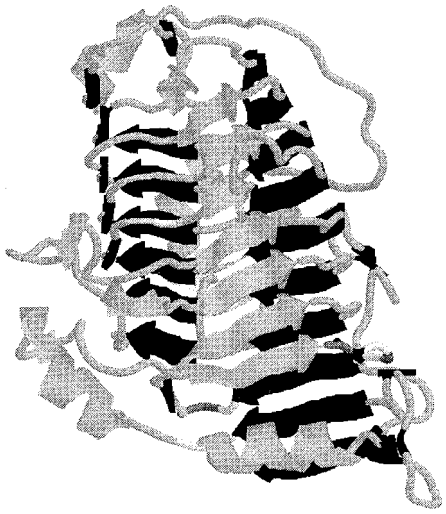

FIGURE 1: Structure of pelC determined by X-ray crystallography (*1*) in a representation generated by RasMol (*56*). The β-helix is highlighted in gray (in front) and black (in back) arrows, and the remaining α-helical and other secondary structures are in gray.

the interior and exterior of the protein, there are several stacks of two or three aromatic and histidine residues. Finally there is a network of aromatic amino acids at the junction between the N and C termini of the protein. The nature of these interactions can provide insight into the role of side-chain interactions in guiding the folding process and their relative contributions to the stability and structural organization of proteins.

The goal of this study is to investigate the physical properties and the folding of wild-type pelC. To understand the folding mechanism and structural organization, we have monitored the equilibrium of chemical and thermal denaturation by circular dichroism (CD), fluorescence, and differential scanning microcalorimetry (DSC). From these experiments, the free energy of unfolding ($\Delta G^{\circ}_{H_2O}$) was determined. We have determined that there are two structural components of pelC that differ in thermal stability, and each one unfolds in a simple two-state manner. These structural units are capable of displaying some degree of independence. Although recently a fragment of the tailspike protein from bacteriophage P22 containing the parallel β-helix domain was isolated and studied along with several mutants (*10, 11*), our study represents the first biophysical characterization of a complete parallel β-helix protein.

MATERIALS AND METHODS

Purification of PelC. PelC was purified from the overexpressing *Escherichia coli* strain HB101 carrying a plasmid bearing the gene for wild-type pelC (pPEL410), using published methods (*12*). The cells were grown for ~48 h at 22−25 °C in Luria−Bertani (LB) media supplemented with 50 μg/mL ampicillin and 1 mM isopropyl-β-D-thiogalactopyranoside (IPTG) at culture initiation. Cells were harvested by centrifugation at 8000*g*. Spheroplasts were prepared by the method of Witholt et al. (*13*).

Cells from a 2 L culture were suspended in 200 mL of 0.2 M Tris-HCl (pH 8.0), and then centrifuged at 8000*g*. The pellet was resuspended in 32 mL of 0.2 M Tris-HCl (pH 8.0). Then 40 mL of 0.2 M Tris-HCl/1 M sucrose and 800 μL of 50 μM EDTA were added. The suspension was mixed well and allowed to stand for 5 min. Eight hundred microliters of fresh hen egg-white lysozyme solution (6 mg/mL) and then 80 mL of distilled water were added, mixed well, and allowed to stand for 20 min at room temperature. The resulting spheroplasts were pelleted by centrifugation at 15000*g*, and the supernatant periplasmic fraction was retained. The supernatant was dialyzed against 5 mM Tris-HCl (pH 8.0) at 4 °C for ~48 h using tubing with an M_r cutoff of 6−8 kDa.

The dialyzed supernatant was applied to a Bio-Rad CM Bio-Gel A cation exchange column in 5 mM Tris-HCl (pH 8.0) at room temperature. The column was washed, and pelC was eluted with a gradient of 0−0.25 M NaCl. Fractions were collected and analyzed for absorbance at 280 nm and pectinolytic activity. Peak pelC fractions were pooled, dialyzed against distilled water, lyophilized, and stored at −20 °C.

Pectinolytic Activity Assay. The assay was performed by the method of Kita et al. (*12*). In a 1 cm path length quartz cuvette, 5 μL of diluted pelC was added to 125 μL of 1% sodium polypectate and 870 μL of 50 mM Bis-Tris-propane, pH 9.5, containing 0.5 mM $CaCl_2$. The increase in absorbance at 232 nm was monitored, corresponding to the cleavage of polypectate. One unit of pectate lyase activity is defined as 1 μmol of product formed per minute (1.73 absorbance units min^{-1}) (*12*).

SDS−PAGE and HPLC were used to assay for protein purity. Mass spectrometry and N-terminal sequencing confirmed the presence of pelC.

Circular Dichroism Spectroscopy. CD spectra of pelC were obtained with a Jasco J-720 spectropolarimeter in cylindrical, water-jacketed quartz cuvettes. The temperature was regulated by circulating water. Protein concentrations were 10−20 μM. Far-UV measurements were made in a 0.01 or 0.02 cm path length cell, and near-UV CD spectra were recorded in a 1 cm path length cell. All concentration measurements were converted to residue concentration by multiplying the protein concentration by the number of amino acid residues. Protein concentrations were determined in 6 M guanidine hydrochloride by UV absorption using a Cary 118 spectrophotometer. A molar extinction coefficient of 61 590 M^{-1} cm^{-1} was calculated using the method of Edelhoch (*14*). All CD spectra were obtained by averaging 20 scans, subtracting a baseline, and converting the raw data to units of molar ellipticity.

Fluorescence Spectroscopy. All fluorescence spectra were collected on an Aviv Instruments (Lakewood, NJ) model ATF-105 differential ratio spectrofluorometer using 1 cm quartz cuvettes and thermoelectric temperature control. PelC was excited at 282 nm, which is the excitation maximum, with an excitation bandwidth of 2 nm and an emission bandwidth of 4 nm. Raw photomultiplier tube signal was converted to sample fluorescence, and a rhodamine-B quantum counter was used to correct for lamp fluctuations. Data were collected at 1 nm steps, and averaged for 1 s per datum. 8-Anilino-1-naphthalenesulfonate (ANS) was used in a molar excess of 200 relative to the protein concentration.

Equilibrium Unfolding Experiments. Individual guanidine hydrochloride (gdn-HCl) solutions were prepared volumetrically as described by Pace (*15*) using ultrapure gdn-HCl purchased from ICN Biomedicals (Costa Mesa, CA). The concentration of a stock solution was determined by the

difference in refractive index between the guanidine solution and the buffer. A 6 M stock solution was diluted in 0.1 M sodium phosphate, pH 7.0 or 5.0, 150 mM sodium chloride to the required final concentration. The necessary volume of a 100 μM protein stock solution was added to the individual gdn-HCl solutions and allowed to equilibrate for 36−48 h with the temperature regulated at 25 °C. Changes in far-UV CD were monitored at 218 nm at 25 °C using a final protein concentration of 10 μM in a 0.1 cm path length cell. Changes in near-UV CD were followed at 277 nm at 25 °C using a final protein concentration of 10 μM in a 1 cm path length cell. For denaturant titrations, changes in tryptophan fluorescence were followed by exciting at 290 nm and monitoring the emission at 326 nm. For fluorescence measurements, protein concentrations were 1 μM.

Chemical Denaturation Data Analysis. Data from gdn-HCl unfolding curves were analyzed assuming a two-state transition, using the linear extrapolation method as described by Pace (*15*). An entire unfolding experiment can be fit to eq 1:

$$y = b_f + (m_f*[\mathrm{Gdn}]) + [b_u + (m_u*[\mathrm{Gdn}])]\frac{\exp((-\Delta G^\circ_{H_2O} + m*[\mathrm{Gdn}])/RT)}{1 + \exp((-\Delta G^\circ_{H_2O} + m*[\mathrm{Gdn}])/RT)} \quad (1)$$

The quantities R and T represent the gas constant and the absolute temperature, respectively; y is the value of any observable parameter (CD, fluorescence, etc.) under specific conditions; b_f and b_u are the y-intercepts of the folded and unfolded baseline, respectively; m_f and m_u are the slopes of the folded and unfolded baselines, respectively; $\Delta G^\circ_{H_2O}$ is the standard free energy of unfolding in water in the absence of denaturant; and m is the change in free energy with denaturant concentration. The constant m has been proposed to be proportional to the change in solvent-exposed surface area with increasing denaturant concentration. It is an indication of the cooperativity of the system. The nonlinear regression function in the program Axum (MathSoft, Inc., Cambridge, MA) was used to fit the experimental data to eq 1. Initial parameter estimates were obtained from linear fits to the folded and unfolded baselines, and a linear fit to the free energy change. Estimated errors are those calculated from the nonlinear regression and represent the standard deviation of the mean.

Calorimetry. Calorimetric measurements were performed with the prototype DASM-4 model microcalorimeter built at The Johns Hopkins University. All calorimetric measurements were conducted at a heating rate of 1 K/min and excess pressure of 1.5 atm. All experiments were performed in buffer solutions with an ionic strength of 20 mM. The protein concentrations in these experiments were varied from 25 to 44 μM depending on solvent conditions and tendencies to aggregate (pH 10, 25 μM; pH 8, 34 μM; pH 7, 37 μM; pH 6, 37 μM; pH 5, 33 μM; pH 4, 28 μM; pH 3, 44 μM). The partial specific heat capacity has been determined according to the procedure described elsewhere (*16*), assuming that the relative molecular mass of pelC is 37.7 kDa and the partial specific volume is 0.726 cm^3/g, calculated from the amino acid composition (*17*). The partial heat capacity of the unfolded polypeptide chain was calculated according to Privalov and Makhatadze (*18*), using the known heat capacity values of amino acid residues.

The calorimetric transition enthalpy, $\Delta H(T_{tr})$, was determined from the area of the heat absorption peak by extrapolating the heat capacity of the initial and final states to the mid-transition temperature, T_{tr}. This is in accordance with the previously determined temperature dependencies of these functions: linear for the native state and polynomial for the unfolded state. The entropy of transition was determined at the transition temperature, T_{tr}, as: $\Delta S(T_{tr}) = \Delta H(T_{tr})/T_{tr}$. A deconvolution analysis of the protein excess heat capacity function was performed using the program based on the sequential procedure of Freire and Biltonen (*19*). The DSC data were fitted assuming a multistate mechanism comprising one or more irreversible steps using software described elsewhere (*20*).

Thermal Denaturation Monitored by CD. Thermal denaturation was carried out, and monitored by far- and near-UV CD on a Jasco J-720 spectropolarimeter equipped with a NESLAB RTE-110 water bath. The rate of change of the temperature was 30 °C/h, controlled by circulating water. Care was taken to ensure that the hoses connecting the water bath to the CD cells were insulated. Data were collected at 0.5 °C intervals. The midpoint of the denaturation curves was determined by taking the second derivative of the curve and using the temperature where the second derivative intersected the zero line.

Analytical Ultracentrifugation. All measurements were made using a Beckman XL-I analytical ultracentrifuge. Samples were prepared identically to those used for the chemical denaturation experiments. Data were collected using concentrations of 5, 10, and 15 μM at 18, 25, and 33 Krpm. The path length of the observation cell was 1.2 cm. Samples were spun for 12 h. Three scans were taken at 2 h intervals. Identical results ensured that equilibrium was achieved. Origin software (Microcal Software Inc., Northhampton, MA) was used to fit the data to a single-species model of association using a partial specific volume of 0.726 cm^3/g.

RESULTS

Sedimentation Analysis. About half of the known parallel β-helix proteins are trimeric (*21*−*25*). Association of the monomeric pelC could lead to deviations from simple two-state behavior and thus to anomalies or complications in a study of protein denaturation. Sedimentation equilibrium experiments were carried out at pH 5 and 7. The results indicate that, under all conditions studied, pelC behaves as an ideal monomer with a relative molecular mass of 38 019 ± 268 Da (data not shown).

Reversibility of Chemical Unfolding. A requirement for thermodynamic analysis of any process is that it is reversible. A logical first step is to show that after unfolding in strongly denaturing conditions the native structure can be completely regained (Figure 2). The far-UV CD spectrum of native pelC is typical of a protein with a high fraction of β-sheet secondary structure. The secondary structure contents of pelC (Table 1) determined from the X-ray structure (*26*) analyzed by the DSSP method (*27*) and from CD using the CDPro secondary structure prediction package (*28*−*31*) differ substantially more than the rms errors normally encountered in this type of analysis (*28*−*31*). The CD secondary structure

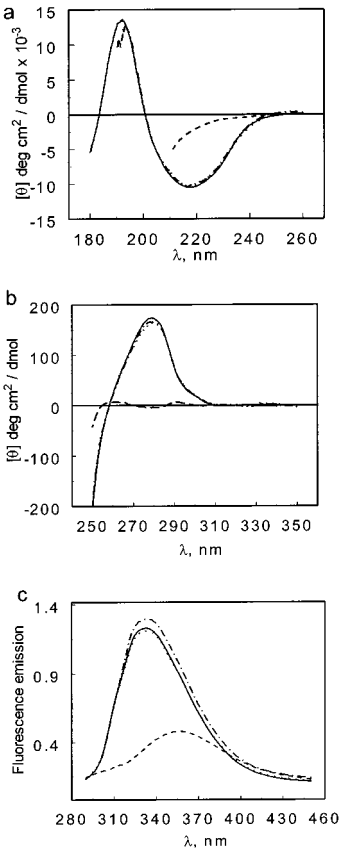

FIGURE 2: Far-UV CD (a), near-UV CD (b), and fluorescence spectra (c) of pelC at pH 7 (—), pH 5 (— · —), pH 7 and 6 M guanidine hydrochloride (— —), and refolded from 6 to 0.6 M guanidine (· · ·). For the far-UV CD, the final gdn-HCl concentration is 0.44 M.

Table 1: Fractions of Secondary Structure in PelC Determined by X-ray Diffraction and Circular Dichroism

	α-helix	β-sheet	turns	other
X-ray[a]	10.7	26.6	4.0	58.7
DSSP[b]	8.8	32.0	7.9	51.3
CDPro[c]	24.3	21.3	22.0	32.5

[a] Estimates from the X-ray diffraction structure (*26*). [b] Objective analysis of the structure from X-ray diffraction using the method of Kabsch and Sander (*27*). [c] Estimation of secondary structure from circular dichroism (*28*−*31*).

analysis uses a reference set of proteins for which the 3D structures and CD spectra are known. The program compares the sample CD spectrum with the reference spectra in the basis set. The secondary structure content is estimated from the known crystal structures in the basis set. Discrepancies arise in the analysis of pelC because this type of protein is not well represented in the reference set used for the secondary structure analysis by CD. In addition, a small shoulder is present at about 225−230 nm (Figure 2a). This shoulder probably arises from aromatic contributions, and it may be responsible for the overestimation of the α-helix content. Figure 2 shows far- and near-UV CD spectra and fluorescence spectra of native, unfolded, and refolded protein. It is clear from this evidence that nativelike secondary structure, tertiary structure, and tryptophan environment are regained upon dilution of gdn-HCl from 6 M to less than 0.6 M. The far-UV CD spectrum shows the broad minimum centered at 218 nm, with an intensity of about −10 500 deg cm^2/dmol (Figure 2a). The CD spectrum of pelC in 6 M gdn-HCl clearly indicates a change in structure. The characteristic broad β-sheet band centered at 218 nm has been lost, and the decreased intensity and band shape are that of a predominantly unordered polypeptide. At 25 °C and 6 M gdn-HCl, there might be a contribution from the polyproline II (PP_{II}) conformation to the CD spectrum. The CD spectrum, which is weakly negative and devoid of features in the 220−230 nm region, suggests such a contribution (*32*). β-Sheet secondary structure is clearly regained upon dilution of 6 M to 0.44 M gdn-HCl.

In the near-UV CD region, the ordered environments of aromatic chromophores and disulfide bonds are responsible for circular dichroism (*33*). The native state is characterized by a broad, positive band centered at about 280 nm which is due to the aromatic side chains, with a small shoulder at about 295 nm possibly arising from disulfide contributions (Figure 2b). The near-UV CD of the fully unfolded state in 6 M gdn-HCl is featureless, and even becomes slightly negative in the 280 nm region. Upon dilution of the denaturant, the native spectral features reappear quantitatively. This indicates that the native arrangement of aromatic side chains of pelC is completely lost at the elevated denaturant concentration and is fully regained upon refolding from the chemically denatured state.

Intrinsic tryptophan and tyrosine fluorescence are good probes of changes in protein conformations. They are sensitive to the degree of solvent exposure, i.e., the polar environment of the aromatic side chains. Native pelC, upon excitation at 282 nm, shows a broad emission band with a maximum at 333 nm (Figure 2c). In 6 M gdn-HCl, a loss of 70% of the intensity is observed, along with a shift in the emission maximum 21 nm to the red to 354 nm. In addition, there is a weak shoulder at about 315 nm. The latter feature is typical of tyrosine fluorescence, and indicates a loss of energy transfer from tyrosine to tryptophan. These changes are consistent with the process of protein unfolding and exposure of buried tryptophan residues to the solvent, as well as an increase in the average distance between tyrosine and tryptophan side chains. The resultant loss of intensity and red shift in tryptophan emission result from solvent quenching (*34*, *35*). After a 10-fold dilution from 6 to 0.6 M gdn-HCl, pelC completely regains the native emission spectrum, indicating that the aromatic side chains are in an environment identical to that of the native conformation.

One of the most convincing arguments for reversibility is the reappearance of enzymatic activity after unfolding. After complete unfolding in 6 M gdn-HCl, and removal of the denaturant by dialysis, the enzymatic activity of pelC is regained and is identical to that of freshly purified pelC, within experimental error (data not shown).

These results indicate that the structure of pelC can be completely disrupted by a chaotropic denaturant and can then be fully recovered upon dilution of the denaturant.

Guanidine Hydrochloride Unfolding of PelC at pH 5 and 7. PelC can be reversibly unfolded by titration with gdn-HCl. Figure 3 shows the changes in the optical properties of pelC at pH 7 upon increasing the denaturant concentration. The molar ellipticity at 218 nm is an indication of the amount of intact β-sheet secondary structure within pelC (Figure 3a). A two-state model of unfolding is assumed for this analysis. A smooth transition occurs upon going from 0 to 3.0 M gdn-

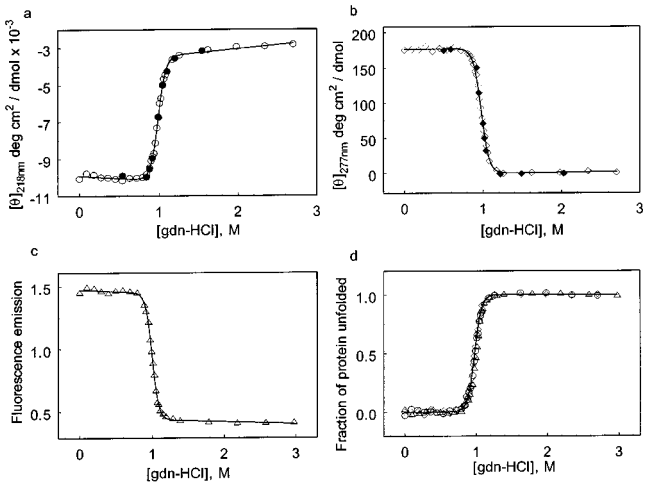

FIGURE 3: Denaturation at pH 7 followed by (a) CD at 218 nm, (b) CD at 277 nm, and (c) fluorescence emission at 326 nm with excitation at 290 nm. The transitions followed by the different probes have been converted to fraction of protein unfolded and are shown in (d). Open symbols represent addition of denaturant to a solution of native protein, and closed symbols are for the dilution of denaturant by buffer.

Table 2: Thermodynamic Results from gdn-HCl Denaturation at pH 7 and 5[a]

pH		218 nm CD	277 nm CD	fluorescence emission
7	$\Delta G°$ (kcal/mol)	12.06 ± 0.59	11.56 ± 0.40	13.03 ± 0.67
	m [kcal/(mol·M)]	12.19 ± 0.59	11.81 ± 0.40	13.04 ± 0.67
	$D_{1/2}$ (M)	0.99 ± 0.1	0.98 ± 0.06	1.00 ± 0.1
5[a]	$\Delta G°$ (kcal/mol)	12.10 ± 0.38	14.92 ± 0.50	14.02 ± 0.67
	m [kcal/(mol·M)]	12.51 ± 0.39	15.70 ± 0.52	14.51 ± 0.70
	$D_{1/2}$ (M)	0.97 ± 0.06	0.95 ± 0.06	0.96 ± 0.1

[a] Because the two-state model on which the analysis is based does not hold at pH 5, these results do not accurately describe the denaturation process at this pH, as indicated by the significant differences between the values obtained from the three spectroscopic probes.

HCl with no indication of intermediate conformations. In the transition region, there are no plateaus or inconsistencies between different physical properties that might imply the existence of intermediates or structural domains. Another important result to note is that an identical curve results from dilution of the denaturant with buffer. The equilibrium value for the CD signal obtained by starting the reaction with either folded or unfolded protein is identical. This indicates that chemical denaturation is thermodynamically reversible and equilibrium is achieved. Another essential feature to notice is the single, highly cooperative transition from the folded to the unfolded state. This allows one to define the equilibrium constant for points in the transition region and to calculate the free energy of unfolding using the linear extrapolation method as described under Materials and Methods (Table 2). These three facts allow us to be confident that thermodynamic parameters extracted from the curves are accurate. This analysis yields $\Delta G°_{H_2O} = 12.06 \pm 0.59$ kcal/mol, $m = 12.19 \pm 0.59$ kcal/(mol·M), and $D_{1/2} = 0.99 \pm 0.1$ M. The native baseline region is linear but shows a slight negative slope. This is probably a result of the molecular structure adjusting to changing solvent conditions resulting from increased ionic strength from the gdn-HCl. The denatured baseline also is linear but has a significant positive slope. This results from increasing amounts of PP_{II} structure within the denatured protein ensemble as the concentration of gdn-HCl is increased at constant temperature.

Figure 3b shows the near-UV CD as a function of gdn-HCl concentration at pH 7. Aromatic side chains are primarily responsible for the near-UV CD. Again there is no concentration range within the transition region where any intermediate conformations are detectable, and the transition is completely reversible. Figure 3b shows the molar ellipticity at 277 nm fit to a two-state model. This unfolding transition is similar to that observed in the far-UV. It is a single smooth transition from the native to the unfolded conformation. In this case, the native and denatured baselines show a negligible slope. Therefore, the only significant change to the aromatic structure occurs in the transition region. A nonlinear least-squares analysis of the data yields results identical, within experimental error, to those obtained from far-UV CD experiments (Table 2).

The same experiment was repeated with fluorescence emission spectroscopy. Figure 3c shows the denaturation process, monitored with excitation at 290 nm and emission at 326 nm, fit to the same two-state model as the CD experiments. This transition is qualitatively similar to the CD-monitored transitions, with a single sharp transition and no intermediate conformations stabilized. In this case, the slopes of the native and denatured baselines result from changing solvent conditions causing an increase in collisional quenching. A nonlinear least-squares analysis of these data also yields results identical to those determined by CD (Table 2).

An important observation is that the transition region appears to occur at similar denaturant concentrations as determined by the three separate probes. Figure 3d shows the three spectral plots converted into fraction of protein unfolded, and fit to the two-state model used in all three unfolding experiments. Indeed, the transitions monitored by the three separate probes are coincident, and to a first approximation, this system can be treated as a two-state process.

PelC has its maximum thermal stability at pH 5 (Table 3, Figure 7b). This is 4 pH units below the isoelectric point (pI = 9). Many proteins exhibit a maximum in thermal stability at or about their pI. We therefore decided to investigate the behavior of pelC at pH 5. In some respects, the results are similar to those obtained at pH 7, but, surprisingly, there were some interesting features that arose when the pH was reduced to 5. Figure 2 shows that at pH 5 and 7, pelC shows similar spectroscopic properties. The far- and near-UV CD and fluorescence spectra are identical when measured for the two pH values. We can conclude that there are no significant perturbations in the structure of native pelC in going from pH 5 to 7. However, there is a change in the denaturation behavior. When denaturation was monitored by far-UV CD (backbone unfolding), there appeared to be virtually no change in the behavior (Figure 4a). However, there was an increase in the overall free energy and the m value of unfolding for the transition when following side-chain properties, such as near-UV CD or fluorescence (Table 2 and Figure 4b,c), but only a small change in the unfolding midpoint, which is the same as for pH 7 within experimental error. The unfolding transition monitored by three probes

Table 3: Thermodynamic Properties of PelC Determined by Differential Scanning Microcalorimetry[a]

pH	T_m (°C)	ΔH_u (kcal/mol)	ΔH_{vH} (kcal/mol)	$\Delta H_{vH}/\Delta H_u$	ΔS_u [kcal/(mol·K)]	ΔH(25 °C) (kcal/mol)	ΔS(25 °C) [kcal/(mol·K)]	ΔG(25 °C) (kcal/mol)	$\Delta C_p(T_{max})$ [kcal/(mol·K)]
8	46.5	235.30	201.09	0.85	0.74	149.30	0.46	12.87	4.00
7	51.2	240.20	219.64	0.91	0.74	150.80	0.45	15.74	3.40
6	56.5	255.30	203.07	0.80	0.77	132.50	0.38	18.33	3.90
5	59.8	270.20	181.67	0.67	0.81	134.50	0.38	20.88	3.90
4	56.5	256.10	174.09	0.68	0.78	130.10	0.38	18.25	4.00
3	51.8	162.00[b]	178.30[b]	1.11[b]	0.50	89.60	0.27	9.67	2.70

[a] T_m is the midpoint temperature, ΔH_u is the calorimetric enthalpy determined by the area under the heat capacity curve, ΔH_{vH} is the van't Hoff enthalpy, ΔS_u is the change in entropy at the transition temperature, ΔG is the free energy of unfolding, and $\Delta C_p(T_{max})$ is the change in heat capacity at the maximum temperature. [b] ΔH_{vH} is greater than ΔH_u at pH 3 because of the large population of unfolded molecules in equilibrium with the folded protein.

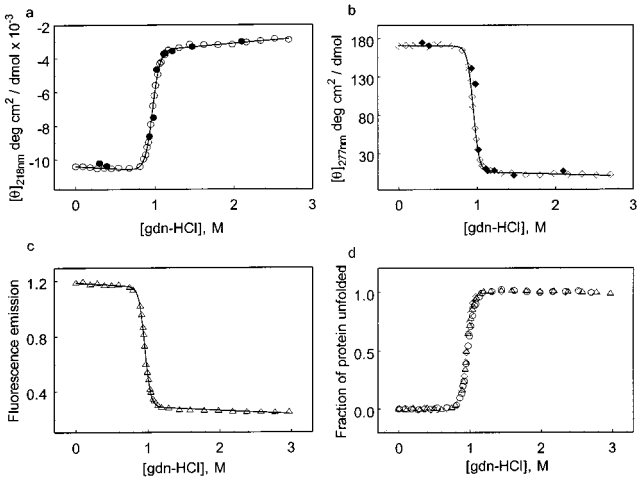

FIGURE 4: Denaturation at pH 5 followed by (a) CD at 218 nm, (b) CD at 277 nm, and (c) fluorescence emission at 326 nm with excitation at 290 nm; the fraction of protein unfolded for each probe is shown in (d). Open symbols represent addition of denaturant to a solution of native protein, and closed symbols are for the dilution of denaturant by buffer.

still appears coincident under these conditions (Figure 4d) despite the differences in the $\Delta G^\circ_{H_2O}$ and m values as measured by the three probes. At pH 7, $\Delta G^\circ_{H_2O}$, m, and $D_{1/2}$ are almost identical when measured by CD and fluorescence. At pH 5, the $\Delta G^\circ_{H_2O}$ value measured by CD at 218 nm is lower than that calculated from the parameters sensitive to side-chain conformation. One still observes what appears to be global unfolding of the protein due to a high degree of cooperation within the protein, as indicated by the apparent coincidence of the unfolding transitions. However, it appears that 277 nm CD and fluorescence are measuring a different transition than 218 nm CD is measuring. The discrepancy between the $\Delta G^\circ_{H_2O}$ and m values from the different spectral probes indicates that at pH 5 there is a decrease in the cooperativity within pelC, and therefore these data do not support a two-state model of denaturation.

We tested the idea that a molten globule intermediate may be responsible for the deviations from apparent two-state behavior at pH 5. When ANS is added to a solution of pelC in acidic buffer (pH <3), a large increase in the fluorescence emission at 500 nm is observed (data not shown). This indicates that ANS is bound in a hydrophobic environment. What is actually happening is that ANS is inducing the formation of ordered structure via electrostatic interactions (manuscript in preparation). Several other lines of evidence indicate that the protein is completely unfolded at pH 2. Calorimetry indicates that there is no cooperative increase

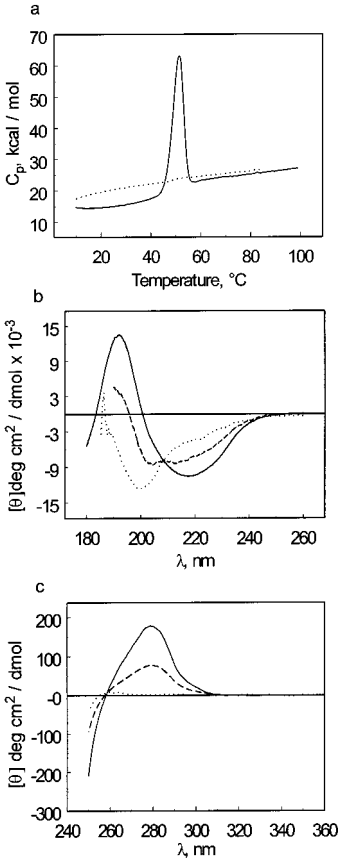

FIGURE 5: Native and acid-denatured pelC. Calorimetric unfolding curves (a) at pH 2.2 (· · ·) and pH 7 (—), (b) far-UV CD spectra at pH 2.2 (· · ·), 3 (- - -), and 7 (—), and (c) near-UV CD spectra at pH 2.2 (· · ·), 3 (- - -), and 7 (—). The CD spectra were collected at 25 °C.

in heat absorption with an increase in temperature (Figure 5a), implying the absence of structure at pH 2. Isoelliptic points in the far-UV CD (at 209 nm, Figure 5b) and the near-UV CD (257 nm, Figure 5c) indicate that pelC exhibits essentially two-state denaturation behavior over the pH range of 2.2−7 at 25 °C. At pH 2.2, the protein is completely unfolded, whereas at pH 3, folded and unfolded proteins are present to a comparable extent. Furthermore, the temperature dependence of the far-UV CD signal indicates that from 0 to 80 °C there is only a modest change in the equilibrium distribution of unordered conformations at pH 2.2, and no cooperative transition is observed (data not shown). The temperature dependence of the CD spectrum at pH 5 and 2 M gdn-HCl also indicates a change from PP_{II} conformation to a more random distribution of structures as the temperature

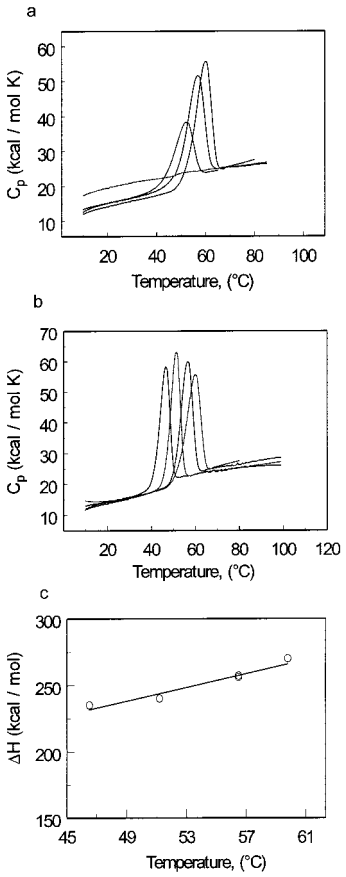

FIGURE 6: Calorimetric unfolding curves for pelC in order of increasing peak height for (a) pH 2.2, 3, 4, and 5 and from left to right for (b) pH 8, 7, 6, and 5. See Table 3 for a summary of the thermodynamic data obtained from these curves. (c) ΔH_{cal} vs temperature indicates that the transition enthalpy increases with increasing temperature.

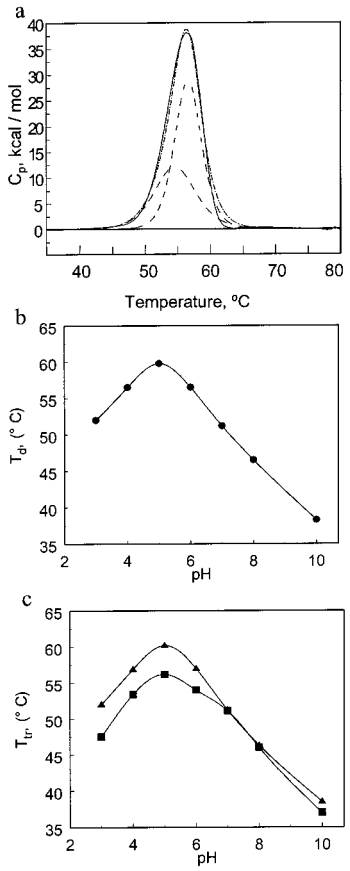

FIGURE 7: (a) Deconvolution analysis of pelC denaturation at pH 6 indicating the experimental curve (—) and deconvoluted component curves (- - -) and the sum of the calculated components (— · —). (b) Observed calorimetric peak maximum as a function of pH. (c) Transition temperatures for the deconvoluted component curves: T_1 (■) and T_2 (▲).

is increased (data not shown), suggesting that there is no residual secondary structure in denatured pelC. Finally, ANS fluorescence was monitored when added to pelC during gdn-HCl titration experiments. At pH 5 and 7, there is no change in ANS fluorescence in gdn-HCl concentrations ranging from 0 to 3.0 M (data not shown). This indicates that no loosely folded intermediate conformations are present at equilibrium during unfolding.

Calorimetric Unfolding of PelC. Figure 6 shows the heat capacity (C_p) as a function of temperature for the irreversible thermal denaturation of pelC (see Discussion). The protein undergoes a cooperative transition accompanied by an increase in heat capacity and extensive heat absorption (ΔH). The denaturation transition appears as a single peak (Figure 6a,b), and upon baseline correction appears to be symmetric (Figure 7a). To a first approximation, denaturation may be treated as a two-state transition. However, the calorimetrically measured enthalpy exceeds the van't Hoff enthalpy, whereas they should be equal for a two-state transition (Table 3). A deconvolution analysis of the curves has been carried out. Under all solvent conditions studied, the denaturation transition can be resolved into two simple two-state transitions. Figure 7a shows the deconvolution of the transition at pH 6, and the two transitions involved. This may mean that pelC contains two structural blocks that strongly cooperate with each other. This cooperativity is so strong that chemical and thermal denaturation appear to be a single cooperative transition at pH 7. Similar observations have been made for the proteins pepsinogen and phosphoglycerate kinase (*36*, *37*).

At first glance, there appears to be an unusual temperature dependence of the heat capacity peaks. The height of the heat absorption peak shows an initial increase, and then decrease with increasing temperature (Figure 6b) that might be interpreted as a decrease of the enthalpy of denaturation with increasing temperature. At the same time, the positive ΔC_p observed upon pelC denaturation requires that the enthalpy change should always increase with increasing temperature. The explanation for the unusual evolution of the heat absorption peaks is in the decrease of the cooperation between the two structural blocks in pelC. Because of this decrease in cooperation within the protein, the integral heat absorption peak of the heat capacity will be broader, and the peak area (calorimetric enthalpy) increases (Table 3, Figure 6c). Figure 7b shows the apparent transition temperature, or, more appropriately, the peak maximum, for pelC. This indicates that the protein's maximum thermal stability is at pH 5. Figure 7c shows that the stability of the structural units is very similar from pH 7 to 8. Above pH 8 and between pH 7 and 5, the difference in thermal stability increases. This means that the structural blocks respond differently to changes in pH, implying some degree of independence. Below pH 5, the difference in thermal stability remains constant with temperature, and the observed decrease in the T_{tr} is a result of the titration of acidic side chains and

Table 4: Thermodynamic Results for the Analysis Assuming Two Two-State Transitions

pH	T_{m_1} (°C)	T_{m_2} (°C)	T_{max} (°C)	ΔH_1 (kcal/mol)	ΔH_2 (kcal/mol)	$\Delta H_{cal}(T_{max})$ (kcal/mol)
8	46	46.3	46.5	81.8	165.1	235.3
7	51.1	51.2	51.2	131.0	135.3	240.2
6	54.0	57.0	56.5	121.0	158.8	255.3
5	56.2	60.2	59.8	111.4	159.5	270.2
4	53.4	56.9	56.5	102.3	136.4	256.1
3	47.5	52.0	51.8	66.5	105.4	162

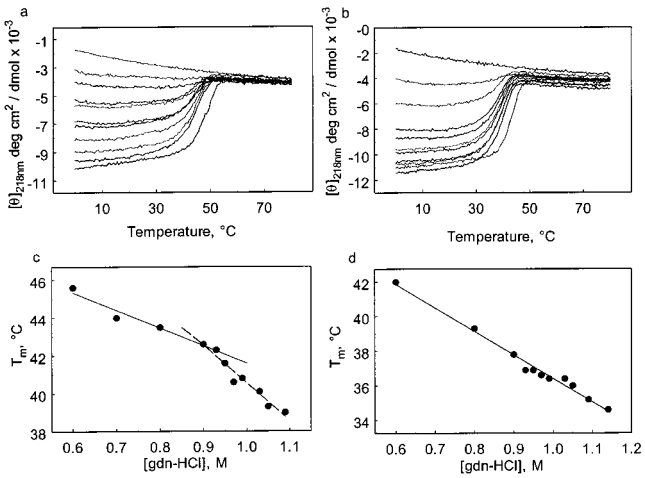

FIGURE 8: Thermal denaturation of pelC monitored by far-UV CD at 218 nm in (a) pH 5 phosphate/NaCl, and (b) pH 7 phosphate/NaCl. Midpoint temperature vs gdn-HCl concentration is shown for (c) pH 5 and (d) pH 7. The curves correspond to gdn-HCl concentrations of 0.6, 0.9, 0.93, 0.95, 0.97, 0.99, 1.03, 1.05, 1.09, 1.14, and 2.0 M reading from bottom to top in the low-temperature region.

stabilization of the unfolded conformation. Tables 3 and 4 give a summary of the thermodynamic data for the overall transition and the two components from the deconvolution analysis, respectively.

CD-Monitored Thermal Denaturation. The results obtained from calorimetry suggest that two cooperative structural blocks are present. The temperature dependence of the far-UV CD signal was therefore examined at pH 5 and 7 in gdn-HCl concentrations corresponding to those in the equilibrium unfolding transition (Figure 8). At high temperatures, pelC solutions less than 0.6 M in gdn-HCl aggregate irreversibly and precipitate. If the time spent at high temperatures is short, the thermal transition of pelC is not accompanied by large effects of irreversibility in gdn-HCl solutions of 0.6 M or greater. PelC undergoes a cooperative transition in all gdn-HCl concentrations in the transition region. It is only at gdn-HCl concentrations exceeding 1.15 M that a transition is not observed. At both pHs and at gdn-HCl concentrations greater than 0.99 M, the initial 218 nm ellipticity at 0 °C is less negative than that at 20 °C. Under these conditions at pH 5, the unordered regions of pelC have a substantial fraction of the PP_{II} conformation. Near-UV CD (Figure 9a) indicates no slope in the baseline from 0 to 20 °C. This indicates that there is no detectable change in the tertiary structure. However, it appears that at pH 7 and temperatures below 25 °C there is a significant positive slope in the near-UV CD baseline (Figure 9b), indicating that the unfolded state becomes populated at low temperatures. The decrease in magnitude of the observed CD signal as the

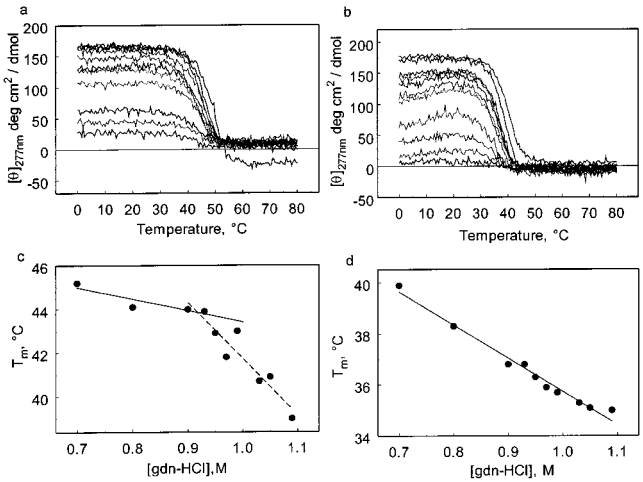

FIGURE 9: Thermal denaturation of pelC monitored by near-UV CD at 218 nm in (a) pH 5 phosphate/NaCl, and (b) pH 7 phosphate/NaCl. Midpoint temperature vs gdn-HCl concentration is shown for (c) pH 5 and (d) pH 7. The curves correspond to gdn-HCl concentrations of 0.7, 0.8, 0.9, 0.93, 0.95, 0.97, 0.99, 1.03, 1.05, 1.09, and 1.15 M reading from top to bottom in the low-temperature region.

temperature is decreased and the unfolded form is favored may result from cold denaturation of pelC at low temperatures. This can lead to decreased cooperation of the protein's internal interactions and deviations from two-state behavior (*37*).

A plot of T_m versus denaturant concentration shows yet another difference in behavior at pH 5 and 7 (Figure 8c,d). At pH 7, the midpoint temperature is a linear function of denaturant concentration, but at pH 5, there is a break in the plot at about 0.9 M gdn-HCl. The T_m is a linear function of gdn-HCl concentrations above and below 0.9 M gdn-HCl, the start of the equilibrium unfolding transition. This evidence supports the notion that there are two structural units and these units behave differently under different pH conditions. At pH 7, these structural units show similar thermal properties, and, therefore, their denaturation processes are not resolved. However, at pH 5, where the structural units show some independence in the transition region, we observe two separate behaviors. In more native conditions ($\leq$0.8 M gdn-HCl), the T_m is linear, but in the transition region there is a loss of cooperation within the molecule causing a change in the behavior of the midpoint temperature. The slope of the T_m dependence is steeper, indicating a loss of stability due to domain independence. In other words, as the gdn-HCl concentration increases, the independence of the structural units also increases. We can conclude that this molecule is very strongly dependent on intramolecular cooperativity for its stability, and, therefore, any loss of this cooperativity results in a concomitant decrease in stability. The same experiments monitored in the near-UV give results that are virtually identical to those from the far-UV (Figure 9c,d). This supports the observation of two simple two-state transitions.

DISCUSSION

Denaturation of PelC. To a reasonable first approximation, gdn-HCl unfolding of pelC at pH 7 can be treated as a two-state process at equilibrium. A single, sharp, and fully reversible denaturation transition is observed, which is

coincident when measured by three different probes. Regardless of the conformational property followed during denaturation, the transition profile is the same. This implies that no intermediate conformations are present that can be detected by the techniques employed. The techniques used are very sensitive to conformations and environments of the backbone and side chains. Quite often, in protein unfolding studies, one observes that the near-UV CD shows that unfolding occurs at a lower denaturant concentration or temperature than that observed by far-UV CD. This is often interpreted as evidence for an intermediate state, but this is not always the case. In the case of pelC, what is observed is somewhat unusual. At pH 7, the transitions induced by chemical and thermal denaturation and monitored by spectroscopic probes suggest that a two-state process accurately describes the transition. Three independent spectroscopic probes yield a coincident chemical denaturation transition as well as thermodynamic parameters that are identical within experimental error. When thermal denaturation in the presence of gdn-HCl is followed by two spectroscopic probes at pH 7, there also appears to be a two-state transition. Although thermal denaturation is only partially reversible, and therefore not a strict equilibrium process, one can still observe the denaturation and approximate the transition midpoint. The dependence of the midpoint temperature on solution conditions is related to structural changes. Under conditions that might stabilize an intermediate or favor a non-two-state process, such as 0.9−1.2 M gdn-HCl, one still observes only a single transition. A plot of the midpoint temperature vs denaturant concentration yields a straight line. This implies that the decrease in midpoint temperature is a result of an overall destabilization of the protein, and it is not due to an increasing population of intermediate structures. The midpoint temperatures at each gdn-HCl concentration are also approximately equal when measured by far- and near-UV CD.

The spectroscopically based observations are contradicted by calorimetry, which indicates that the overall unfolding process is not a two-state transition, but can be resolved into two separate two-state transitions. A true test of a two-state process can be made using calorimetry. The ratio of the van't Hoff enthalpy to the true calorimetric enthalpy ($\Delta H_{vH}/\Delta H_{cal}$) for a two-state process is 1. Typically an experimental error of ±5% is allowed (*38*). For pelC at pH 7, this ratio is 0.91. This value is close to 1, but it is sufficiently outside of the margin of error such that one is unable to assume a two-state transition. Under all other solvent conditions examined with calorimetry, the two-state model fails even more conclusively (Table 3). The existence of an equilibrium intermediate is not supported by our spectroscopic data. However, the spectroscopic and calorimetric data support the presence of two structural blocks or cooperative units. The molecule's overall stability suggests an unusually high degree of cooperativity between these structural blocks, which makes the denaturation appear as a two-state process. The deconvolution of the calorimetric denaturation data yields the two transitions implied by the ratio of van't Hoff and calorimetric enthalpies (Figure 7).

Although thermodynamic analysis can generally be applied only to reversible transitions, it can also be employed for partially reversible processes, if some calorimetric criteria are satisfied (*16*). The formalism of equilibrium thermodynamics can be used to analyze scanning calorimetry data if the irreversible part of the transition does not exhibit measurable exothermic effects during and after the transition. It was noted that changes in the heat capacity function in this case do not affect the shape of the calorimetric curve, which exhibits a Gaussian shape similar to reversibly denaturing proteins under similar solvent conditions. The heat capacity increment of denaturation often appears unaffected if exothermic effects due to aggregation are absent. Usually these characteristics apply to those proteins that have denaturation transitions that are only partially reversible judging by the calorimetric criteria. In some cases, the degree of the reversibility of the denaturation transition strongly depends on the temperature to which the protein has been heated. With a decrease in the maximum temperature to which the protein has been exposed, many proteins exhibit calorimetric profiles such as those expected in the absence of an exothermic effect of aggregation. This allowed us to apply thermodynamic analysis, with some restrictions, to obtain denaturation parameters of pelC. In all cases, we tested for sources of irreversibility that might affect the structural and thermodynamic characteristics of its thermal unfolding. According to established criteria, based on Lumry−Eyring models (*39*), pelC can be classified as a type-A irreversible system (*40*) (data not shown); i.e., equilibrium thermodynamic analysis is permissible.

Denaturation was also studied at pH 5 where deviations from the two-state model are most prominent. Under these conditions, differences in the apparent $\Delta G°$ and m values that cannot be accounted for by experimental error are obtained using different spectroscopic parameters. The denaturation transitions still appear to be nearly coincident, but the analysis of the thermodynamic data obtained indicates that the two-state model fails (Table 2). These results would suggest that the free energy change measured from the backbone denaturation is less than that measured from the side chains, which is not permitted under the constraints of the two-state model. Therefore, the two-state model cannot accurately be applied at pH 5, and the thermodynamic parameters derived from the spectroscopic analysis are not accurate.

Calorimetry suggests that, under these conditions, two separate two-state transitions exist, and at pH 5 the individual transitions show the most independence and the individual transition temperatures have the greatest difference. If we follow the thermal denaturation by CD at various gdn-HCl concentrations, we see that there is a nonlinear dependence of the midpoint temperature. At denaturant concentrations within the transition region, the slope of the T_m vs denaturant concentration becomes more negative, suggesting an enhanced dependence of stability on denaturant concentration. This decrease in stability results from a loss of intramolecular cooperativity, which supports the idea that there are two individual two-state transitions. This is further supported by the data from the near-UV CD that show a similar break in the midpoint dependence (Figures 8 and 9).

Several lines of evidence suggest that these anomalies are not due to a partially structured intermediate. These include the lack of secondary and tertiary structure at pH 2.2 over a wide range of temperatures. Although ANS binds to pelC at pH 2.2, as indicated by a large increase in fluorescence emission, this is due to the formation of ordered secondary

structure induced by ANS binding (*41*, and manuscript in preparation). If a structured intermediate state can exist at extreme pH conditions, this would imply that a similar structured state could also exist in an equilibrium denaturation situation. The absence of a thermal transition in 2 M gdn-HCl also indicates that there is no ordered structure remaining in the unfolded ensemble. In addition, no ANS binding occurs in the gdn-HCl-induced unfolding transition. Last, far- and near-UV CD indicate that the loss of secondary structure due to acid denaturation parallels the loss of tertiary structure under identical conditions.

There are three lines of evidence that indisputably preclude the possibility of a two-state process. The ratio of the van't Hoff to calorimetric enthalpy is less than 1. Gdn-HCl denaturation at pH 5 using three independent spectroscopic probes yields inconsistent values for $\Delta G°$. Finally, thermal denaturation at pH 5 exhibits a nonlinear dependence of the midpoint temperature on denaturant concentration.

The results discussed can be applied to the protein folding phenomena in a more general sense. The existence of two cooperative units that are not at all obvious in the crystal structure, and are also rather elusive to spectroscopic probes, implies that the results obtained in this study may not be unique. It would be rather surprising if a relatively large protein, such as pelC, folded via a simple two-state mechanism. Consequently, larger proteins that do exhibit apparent two-state behavior may very well be composed of closely interrelated structural blocks whose independence and existence require a detailed characterization in order to be elucidated.

Stability of PelC. PelC contains 3 relatively large parallel β-sheets, consisting of 6, 8, and 10 strands per sheet. This protein has a free energy of unfolding that places it among the most stable globular proteins characterized (*42*). It has been reported that β-sheets attain maximum stability with five or more strands (*43*). This may be due to cooperative effects. Strands on the edge of the sheet are only hydrogen-bonded on one side. By increasing the number of strands in a β-sheet, it is possible to increase the overall stability by increasing the cooperative stability of the internal strands. Side-chain interactions probably play a role in the high stability of pelC as well. Stacks of aliphatic amino acids are arranged in a linear fashion, with C_α distances spaced at an optimal 4.5−5.5 Å (*1*). These residues form a highly ordered, compact hydrophobic core with many van der Waals contacts. In addition, stacks of aromatic residues are observed in pelC. These rings are stacked in a face-to-face fashion with a slight offset. This allows for optimum orientation of ring hydrogens and π orbitals. Betts and co-workers have shown that aromatic stacks in P22 tailspike protein (TSP) are important for stability and specificity (*44*). It has been suggested that parallel β-sheets are less stable than antiparallel sheets (*45*). This is because parallel sheets are often found buried and it has been inferred that they cannot tolerate solvent access to their hydrogen bonds. Theoretical calculations indicate that this is in fact due to less effective interchain packing and less favorable interchain electrostatic interactions (*46*). However, in the case of pelC, the high stability may be a result of efficient side-chain packing resulting from the β-helix fold. Calorimetric measurements imply the existence of two structural units, each of which gives rise to a simple two-state transition. The high degree of cooperation between these units is a major contributor to the high stability of the protein. It should be noted that the free energy reported ($\Delta G°_{H_2O}$) is the free energy of unfolding and represents the work necessary to unfold the entire protein. The stability of the native state would be equal to the stability of the least stable structural component. In pelC, this value is difficult to measure because there is no apparent symmetry that might indicate two energetically similar units, and the structural blocks have not been identified.

The most striking result from chemical denaturation experiments is the large *m* value. In a survey of 16 proteins for which *m* values have been measured, the largest being a 47 kDa fragment of the P22 tailspike protein (*10*), a range of 1.2−4.4 kcal/(mol·M) has been observed (*47*−*53*). PelC exhibits an *m* value of 12 kcal/(mol·M) at pH 7, a value 3-fold greater than any observed in the survey. A similarly structured and much larger protein, TSP from phage P22, yields an *m* value of 3 kcal/(mol·M) (*10*). This *m* value was measured from urea denaturation, which typically yields a lower *m* value than gdn-HCl denaturation (*54*). Empirical relationships have been developed that can be used to estimate the *m* value for gdn-HCl denaturation from experimentally determined *m* values by urea denaturation (*54*). Thus, for TSP, $m_{\text{gdn-HCl}}$ is approximately 6.8 kcal/(mol·M). There are several ways to explain the large value for pelC. From the X-ray structure, there are no significantly exposed loops or elements of secondary structure that would enhance solvent exposure in the folded form. The number of β-strands per sheet may also be responsible for the large *m* value, as the number of strands can influence the cooperativity of the system (*43*). Because of the high $\Delta G°$ value and the low midpoint of unfolding (about 1 M gdn-HCl), a strong driving force is required to favor the folded conformation. Perhaps the largest contributor to the high *m* value is the strong cooperation between structural units. It should be noted that all the proteins in this survey are less than half as large as pelC, except TSP, which is larger and represents only a fragment of the entire protein. Additionally, due to the relatively large size of pelC, many of its residues are buried when folded. Upon unfolding, there is a large change in the solvent-accessible surface area. Using the DSSP program (*27*), the solvent-accessible surface area (ASA) was calculated for both the folded and unfolded forms. Coordinates for an unfolded polypeptide chain with the pelC sequence were generated using β-sheet ϕ and ψ angles with Insight II software (Molecular Simulations Inc., San Diego, CA). To include the effects of disulfide bonds, a simple energy minimization was performed with the two native disulfide bonds of pelC intact. The difference in accessible surface area between the folded and unfolded chains (ΔASA) is 35 189 Å^2 without disulfides and 30 701 Å^2 with disulfides intact. It has been shown that ΔASA, *m*, and ΔC_p correlate well with each other for small proteins that exhibit two-state folding (*54*). In the case of pelC, ΔASA is about what one would expect for unfolding of a protein of its size. However, the experimental value for *m* is higher than what one would expect [calculated value = 8.0 kcal/(mol·M)], and ΔC_p [calculated value = 6.0 kcal/(mol·K)] is lower (*54*). Although this correlation has been established for small, two-state proteins (*54*), it is still useful as a guideline in our situation. A recent study of the denaturation of maltose binding protein reported a comparable *m* value of 12 kcal/(mol·M) (*55*). The

protein denatures via a two-state mechanism, and, therefore, *m* was correlated with its large ΔC_p. In our case, a large *m* is accompanied by a ΔC_p lower than the expected value for a protein the size of pelC. Our results indicate that for proteins such as pelC, which unfold via a mechanism more complex than a simple two-state process, the *m* value may show a different dependence on ΔC_p and ΔASA and/or depend on additional properties.

Some preliminary experiments permit speculation regarding the molecular nature of the two structural blocks and the folding/unfolding mechanism of pelC. Trypsin digestion yields a fragment with a relative molecular mass of approximately 19 kDa, and several small fragments. The 19 kDa fragment's N-terminal sequence is that of intact pelC (unpublished results). In addition, kinetic folding and unfolding experiments indicate that the backbone folds and unfolds in a single cooperative step (unpublished results). This may suggest that there are multiple nucleation sites for folding or unfolding. Energetically, the individual transitions are resolved, but folding and unfolding occurs very rapidly and very cooperatively. Future studies will include isolation and solution conformation determination by NMR of the 19 kDa fragment. Calorimetry of the fragment will also be performed for comparison with the results for the individual denaturation transitions. Kinetic studies of $^1H/^2H$ exchange during folding will also be examined.

When the X-ray structure of pelC was solved, it yielded a novel conformation. Denaturation studies thus far imply the existence of a novel folding mechanism. It appears that two structural units are present in pelC and the cooperativity between them is so strong that unfolding at first appears as a two-state process. This high cooperativity may contribute to the remarkable stability of this protein. Kinetic experiments on pelC folding and unfolding have been initiated and will add to our understanding of the unique folding properties of parallel β-helix proteins.

ACKNOWLEDGMENT

We thank Prof. Noel T. Keen for generously providing clones of pelC. The Beckman XL-I was purchased with an NIH multi-user equipment grant to Colorado State University.

REFERENCES

1. Yoder, M. D., Keen, N. T., and Jurnak, F. (1993) *Science 260*, 1503−1507.
2. Yoder, M. D., Lietzke, S. E., and Jurnak, F. (1993) *Structure 15*, 241−251.
3. Lietzke, S. E., Yoder, M. D., Keen, N. T., and Jurnak, F. (1994) *Plant Physiol. 106*, 849−862.
4. Pickersgill, R., Jenkins, J., Harris, G., Nasser, W., and Robert-Baudouy, J. (1994) *Nat. Struct. Biol. 1*, 717−723.
5. Emsley, P., Charles, I. G., Fairweather, N. F., and Isaacs, N. W. (1996) *Nature 381*, 90−92.
6. Mayans, O., Scott, M., Connerton, I., Graveson, T., Benen, J., Visser, J. Pickersgill, R., and Jenkins, J. (1997) *Structure 5*, 677−689.
7. Barras, F., van Gijsegem, F., and Chatterjee, A. K. (1994) *Annu. Rev. Phytopathol. 32*, 201−234.
8. Tamaki, S. J., Gold, S., Robeson, M., Manulis, S., and Keen, N. T. (1988) *J. Bacteriol. 170*, 3468−3478.
9. Rao, M. N., Kembhavi, A. A., and Pant, A. (1996) *Biochem. J. 319*, 159−164.
10. Miller, S., Schuler, B., and Seckler, R. (1998) *Biochemistry 37*, 9160−9168.
11. Schuler, B., and Seckler, R. (1998) *J. Mol. Biol 281*, 227−234.
12. Kita, N., Boyd, C. M., Garrett, M. R., Jurnak, F., and Keen, N. T. (1996) *J. Biol. Chem 271*, 26529−26535.
13. Witholt, B., Boekout, M., Brock, M., Kingma, J., Heerikhuizen, H., and Leij, L. (1976) *Anal. Biochem. 74*, 160−170.
14. Edelhoch, H. (1967) *Biochemistry 6*, 1948−1954.
15. Pace, C. N. (1988) in *Protein Structure: A Practical Approach*, pp 311−330, IRC Press, New York.
16. Privalov, P. L., and Potekhin, S. A. (1986) *Methods Enzymol. 131*, 4−51.
17. Durchschlag, H. (1986) in *Thermodynamic Data for Biochemistry and Biotechnology*, p 45, Springer-Verlag, New York.
18. Privalov, P. L., and Makhatadze, G. I. (1990) *J. Mol. Biol. 213*, 385−391.
19. Biltonen, R. L., and Freire, E. (1978) *CRC Crit. Rev. Biochem. 5*, 85−124.
20. Freire, E., van Osdol, W. W., Mayorga, O. L., and Sanches-Ruiz, J. M. (1990) *Annu. Rev. Biophys. Biophys. Chem. 19*, 159−188.
21. Steinbacher, S., Seckler, R., Miller, S., Steipe, B., Huber, R., and Reinemer, P. (1994) *Science 265*, 383−386.
22. Raetz, C. R., and Roderick, S. L. (1995) *Science 270*, 997−1000.
23. Kisker, C., Schindelin, H., Alber, B. E., Ferry, J. G., and Rees, D. C. (1996) *EMBO J. 15*, 2323−2330.
24. Beaman, T. W., Binder, D. A., Blanchard, J. S., and Roderick, S. L. (1997) *Biochemistry 36*, 489−494.
25. Beaman, T. W., Sugantino, M., and Roderick, S. L. (1998) *Biochemistry 37*, 6689−6696.
26. Sieber, V., Jurnak, F., and Moe, G. R. (1995) *Proteins: Struct., Funct., Genet. 23*, 32−37.
27. Kabsch, W., and Sander, C. (1983) *Biopolymers 22*, 2577−2637.
28. Provencher, S. W., and Glöckner, J. (1981) *Biochemistry 20*, 33−37.
29. Sreerama, N., and Woody, R. W. (1993) *Anal. Biochem. 209*, 32−44.
30. Sreerama, N., Venyaminov, S. Y., and Woody, R. W. (1999) *Protein Sci. 8*, 370−380.
31. Johnson, W. C. (1999) *Proteins: Struct., Funct., Genet. 35*, 307−312.
32. Sreerama, N., and Woody, R. W. (1994) *Biochemistry 33*, 10022−10025.
33. Woody, R. W., and Dunker, A. K. (1996) in *Circular Dichroism and the Conformational Analysis of Biomolecules* (Fasman, G. D., Ed.) pp 109−157, Plenum Press, New York.
34. McMahon, L. P., Colucci, W. J., McLaughlin, M. L., and Barkley, M. D (1992) *J. Am. Chem. Soc. 114*, 8442−8448.
35. Chen, Y., and Barkley, M. D. (1998) *Biochemistry 37*, 9976−9982.
36. Mateo, P. L., and Privalov, P. L. (1981) *FEBS Lett. 123*, 189−192.
37. Griko, Y. L., Venyaminov, S. Y., and Privalov, P. L. (1989) *FEBS Lett. 244*, 276−278.
38. Privalov, P. L. (1979) *Adv. Protein Chem. 33*, 167−241.
39. Lumry, R., and Eyring, H. (1954) *J. Phys. Chem. 58*, 110−120.
40. Sanchez-Ruiz, J. M. (1992) *Biophys. J. 61*, 921−935.
41. Ali, V., Prakash, K., Kulkarni, S., Ahmad, A., Madhusudan, K. P., and Bhakuni, V (1999) *Biochemistry 38*, 13635−13642.
42. Creighton, T. E. (1993) in *Proteins: Structures and Molecular Properties*, 2nd ed., W. H. Freeman and Company, New York.
43. Sheridan, R. P., Lee, R. H., Peters, N., and Allen, L. C. (1979) *Biopolymers 18*, 2451−2458.
44. Betts, S. D., Kreisberg, J. F., and King, J. (1999) *Biophys. J. 76*, A142.
45. Richardson, J. S. (1977) *Nature 268*, 495−500.
46. Chou, K. C., Pottle, M., Nemethy, G., Ueda, Y., and Scheraga, H. A. (1982) *J. Mol. Biol. 162*, 89−112.
47. Reid, K. L., Rodriguez, H. M., Hillier, B. J., and Gregoret, L. M. (1998) *Protein Sci. 7*, 470−479.

48. Hu, C., Sturtevant, J. M., Thomson, J. A., Erickson, R. E., and Pace, C. N. (1992) *Biochemistry 31*, 4876−4882.
49. From, N. B., and Bowler, B. E. (1998) *Biochemistry 37*, 1623−1631.
50. Kuwajima, K., Garvey, E. P., Finn, B. E., Matthews, C. R., and Sugai, S. (1991) *Biochemistry 30*, 7693−7703.
51. Ahmad, F., and Bigelow, C. G. (1982) *J. Biol. Chem. 257*, 12935−12938.
52. Ahmad, F., and Bigelow, C. G. (1986) *Biopolymers 25*, 1623−1633.
53. Haezebrouck, P., Noyelle, K., and Van Dael, H. (1998) *Biochemistry 37*, 6772−6780.
54. Myers, J. K., Pace, C. N., and Scholtz, J. M. (1995) *Protein Sci. 4*, 2138−2148.
55. Sheshadri, S., Lingaraju, G. M., and Varadarajan, R. (1999) *Protein Sci. 8*, 1689−1695.
56. Sayle, R. A., and Milner-White, E. J. (1995) *Trends Biochem. Sci. 20*, 374−376.

BI001900V